Inorganic Chemistry
Article
pubs.acs.org/IC

Single- and Mixed-Linker Cr-MIL-101 Derivatives: A High-Throughput Investigation

Martin Lammert,[†] Stephan Bernt,[†] Frederik Vermoortele,[‡] Dirk E. De Vos,[‡,§] and Norbert Stock*,[†]

[†]Institut für Anorganische Chemie, Christian-Albrechts-Universität zu Kiel, Max-Eyth-Straße 2, D-24118 Kiel, Germany
[‡]Centre for Surface Chemistry and Catalysis, Katholieke Universiteit Leuven, Arenbergpark 23, B-3001 Leuven, Belgium

Ⓢ *Supporting Information*

ABSTRACT: New single- and mixed-linker Cr-MIL-101 derivatives bearing different functional groups have been synthesized. The influence of the reaction parameters, such as metal source (CrO_3, $CrCl_3$, and $Cr(NO_3)_3{\cdot}9H_2O$) or linker composition, on product formation have been investigated using high-throughput methods. Highly crystalline Cr-MIL-101 materials were obtained with $CrCl_3$ as the metal source with either 2-bromoterephthalic (TA-Br) or 2-nitroterephthalic (TA-NO_2) acid as one of the mixed-linker components. On the basis of these results, numerous new mixed-linker Cr-MIL-101 derivatives containing -NH_2, -NO_2, -H, -SO_3H, -Br, -OH, -CH_3, and -COOH have been synthesized. The use of TA-NH_2 and TA-OH were shown, under the same reaction conditions, to lead to decarboxylation and the formation of 3-amino- and 3-hydroxybenzoic acid, respectively. Furthermore, we were also able to directly synthesize single-linker Cr-MIL-101-X derivatives with X = F, Cl, Br, CH_3. Postsynthetic modification was used to selectively reduce the mixed-linker compound Cr-MIL-101-Br-NO_2 to Cr-MIL-101-Br-NH_2. To establish the successful incorporation of the linker molecules and possible decomposition of certain starting materials, ^1H NMR spectra of dissolved reaction products were recorded.

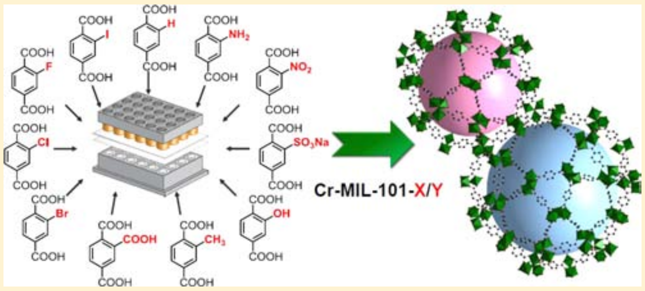

■ INTRODUCTION

In recent years, metal−organic frameworks (MOFs) have gained widespread attention due to their considerable physical and chemical properties.[1] By the choice of the organic building unit (linker), the pore size,[2] specific surface area,[3] and chemical functionality[4] can be varied. MOFs have been studied in different research areas such as catalysis,[5] gas storage,[6] gas separation,[7] drug release,[8] and heat transformation applications.[9] It has been shown that the introduction of different functional groups influences the specific surface area of MOFs[10] and their breathing behavior, such as in Al-MIL-53-X,[4] Fe-MIL-53-X,[11] and Fe-MIL-88-X[12] (X = functional group). The properties can be fine-tuned by using mixtures of linker molecules bearing different functional groups, leading to mixed-linker MOFs.[13] Although some functionalized MOFs can be obtained directly by replacing the unfunctionalized linker by the desired functionalized linker, this is not always easily accomplished. Especially in the case of compounds that are synthesized at high temperatures, some functional groups cannot be incorporated because the starting material decomposes or functional groups are substituted during the synthesis. These groups can be introduced and further modified via postsynthetic modification (PSM).[14] This has previously been shown by the introduction of amino groups, which were reacted with alkyl isocyanates to obtain the corresponding urea derivative[15] or with phosgene/thiophosgene to yield the isocyanate/thioisocyanate derivative.[16]

For the possible applications of MOFs, high thermal and chemical stability is preferable. The compound Cr-MIL-101, $[Cr_3(OH)(H_2O)_2(\mu_3\text{-}O)(O_2CC_6H_4CO_2)_3]{\cdot}nH_2O$, is outstanding for its high thermal stability up to 270 °C as well as its chemical stability.[17] It forms a zeotypic MTN network as observed in the zeolite ZSM-39 with two types of mesoporous cages: dodecaedric cages (5^{12}) with a 29 Å diameter and hexacaidecaedric cages ($5^{12}6^4$) with a 34 Å diameter (Figure 1). The cages are accessible through five-membered (12 Å) and six-membered (16 Å) windows.

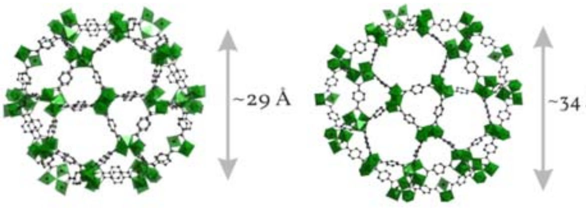

Figure 1. Two types of cages observed in Cr-MIL-101: dodecaedric cages containing five-membered rings (left) and hexacaidecaedric cages containing five-membered and six-membered rings (right).[17]

Received: March 1, 2013
Revised: June 19, 2013
Accepted: June 19, 2013
Published: July 5, 2013

Although Cr-MIL-101 exhibits these striking properties, just a few functionalized derivatives of MIL-101 are known: the amino and nitro derivatives,[15,18−20] the sulfonic acid derivative,[21] and the sulfate derivative.[22] Very recently, the PSM of Cr-MIL-101-NH_2 to the iodo and fluorine derivatives and the introduction of photoswitchable groups was described.[23,24] In comparison to the large number of known derivatives for MIL-53 and MIL-88, the number of incorporated functional groups is limited. In addition, no mixed-linker Cr-MIL-101 compounds have been reported up until now. This is probably due to the unpredictable synthesis conditions that have to be established for every new linker or mixed-linker system.

An efficient way for the simultaneous investigation of a wide parameter range is the high-throughput (HT) methodology.[25] It is based on the miniaturization of conventional hydrothermal reactions where reactions take place in a reactor block with 24 (2 mL volume each) or 48 (300 μL volume each) Teflon inserts. This process allows the simultaneous investigation of several synthesis parameters, such as stoichiometry of reactants or variation of pH. On the other hand, the amount of reactants that are used is drastically reduced compared to that of conventional hydrothermal syntheses. Therefore, HT methods are useful for the discovery of new phases and the subsequent synthesis optimization.

Here, we report the high-throughput investigation of single- and mixed-linker systems in order to get new functionalized Cr-MIL-101 derivatives.

■ EXPERIMENTAL SECTION

Materials. Chromium nitrate (99%, $Cr(NO_3)_3{\cdot}9H_2O$, Honeywell Riedel-de Haën), chromium oxide (99%, CrO_3, Merck), and chromium chloride (99%, $CrCl_3$, Aldrich) were used as obtained. Terephthalic acid (98%, TA-H, Aldrich), 2-aminoterephthalic acid (98%, TA-NH_2, Aldrich), 2-nitroterephthalic acid (98%, TA-NO_2, Fluka), 2-bromoterephthalic acid (95%, TA-Br, Aldrich), 2-hydroxyterephthalic acid (97%, TA-OH, Aldrich), monosodium-2-sulfoterephthalic acid (98%, TA-SO_3Na, ABCR), 2-methylterephthalonitrile (98%, Aldrich), dimethyl-2-fluoroterephthalate (96%, Aldrich), dimethyl-2-iodoterephthalte (98%, Aldrich), 2-chloro-1,4-dimethylbenzene (99%, Aldrich), and sodium hydroxide were used without any further purification. 1,2,4-Benzenetricarboxylic acid (98%, TA-COOH) was received from TCI, and tin(II) chloride (99%, $SnCl_2$) and sodium nitrite (99%, $NaNO_2$) were received from Merck. Potassium iodide (99%, KI) was received from Grüssing.

The linker molecules TA-CH_3, TA-F, TA-Cl, and TA-I were synthesized as described in the Supporting Information.

NMR spectra were measured on a Bruker DRX 500 spectrometer. Sorption experiments were performed using a Bel Japan, Inc. Belsorp$_{max}$ instrument. IR spectra were measured on a Bruker ALPHA-FT-IR A220/D-01 spectrometer equipped with an ATR-unit. PXRD data was recorded on a Stadi P Combi diffractometer with Cu Kα_1 radiation equipped with an image-plate detector system and an *xy*-stage.

Most of the syntheses were carried out in HT reactors with a maximum volume of 2 mL each.[25] The synthesis scale-up of selected single- and mixed-linker Cr-MIL-101 derivatives to reactors with a volume of 40 mL was also accomplished, but not all syntheses were scaled up. We are aware of the fact that the scale-up of reactions is not easily accomplished, and for some reported syntheses, procedure adjustment of the reaction parameters will probably be necessary.

High-Throughput Metal-Source Screening. For the systematic investigation of the influence of the metal sources on the product formation, a reactor block with 24 Teflon inserts was used.[25] The terephthalic acid derivatives were always used in a molar ratio of 1:1. $Cr(NO_3)_3{\cdot}9H_2O$ and CrO_3 were used as aqueous solutions (1.25 M), and $CrCl_3$ was used as a solid. In each Teflon insert, 125 μmol of the chromium source and 125 μmol of the terephthalic acids, or equimolar mixtures adding up to 125 μmol, were introduced. The Teflon reactors were initially filled with the solids (terephthalic acid derivatives, $CrCl_3$) followed by the liquids (metal solution ($Cr(NO_3)_3{\cdot}9H_2O$ or CrO_3), water (1 mL), HCl (250 μmol)). The reactor block was covered with Teflon foil, sealed with the top plate of the reactor, and heated in an oven at 180 °C for 96 h. After the reaction time, the solid was filtered and washed with 500 μL of demineralized water and 500 μL of ethanol. Afterward, the solid was dried in air at 70 °C. The samples were automatically characterized using a STOE HT X-ray powder diffractometer. Details of the high-throughput metal screening experiment are given in the Supporting Information (Tables S1−S3).

High-Throughput Synthesis of Br- and NO_2-Containing Mixed-Linker Cr-MIL-101 Derivatives. For all syntheses, a reactor block with 24 Teflon inserts (2 mL volume each) was used. The starting materials 125 μmol of $CrCl_3$ and 125 μmol of ligand (equimolar mixture of two derivatives) were introduced into the Teflon liners. After the addition of 1 mL of demineralized water, the reactor block was sealed and heated to 180 °C within 1 h. After holding the temperature for 120 h, the reactor block was cooled to room temperature within 6 h. The green solid was centrifuged and redispersed in 20 mL of water (this process was repeated two times with water and three times with ethanol). The resulting green solid was dried in air at 70 °C. Details of the experiments using $CrCl_3$ as the metal source are given in the Supporting Information (Table S4).

Synthesis Scale-Up of the Mixed-Linker Cr-MIL-101 Derivatives Cr-MIL-101-Br-COOH and Cr-MIL-101-NO_2-COOH. The starting materials $CrCl_3$ (198 mg, 1.25 mmol) and 1.25 mmol of ligand (equimolar mixture of the two derivatives) were introduced into a 40 mL Teflon reactor. After the addition of 5 mL of demineralized water, the reactor was sealed and heated to 180 °C within 1 h. The temperature was held for 96 h and cooled to room temperature within 6 h. The green solid was centrifuged and redispersed in 20 mL of water (this process was repeated two times with water and three times with ethanol). The resulting green solid was dried in air at 70 °C. PXRD patterns of the scaled-up products are given in the Supporting Information (Figure S1).

Optimized Synthesis Conditions for Single-Linker Cr-MIL-101 Derivatives. *Synthesis of Cr-MIL-101-CH_3.* For the synthesis, a reactor block with 24 Teflon inserts (2 mL volume each) was used. The starting materials $CrCl_3$ (19.8 mg, 125 μmol) and TA-CH_3 (22.5 mg, 125 μmol) were introduced into the Teflon liner. After the addition of 1 mL of demineralized water, the reactor block was sealed and heated to 180 °C within 1 h. After holding the temperature for 96 h, the reactor block was cooled to room temperature within 3 h. The green solid was centrifuged and redispersed in 20 mL of water (this process was repeated two times with water and three times with ethanol). The resulting green solid was dried in air at 70 °C.

Synthesis of Cr-MIL-101-F. For the syntheses, a reactor block with 24 Teflon inserts (2 mL volume each) was used. The starting materials $CrCl_3$ (19.8 mg, 125 μmol) and TA-F (23.0 mg, 125 μmol) were introduced into the Teflon liners. After the addition of 950 μL of demineralized water and 50 μL of a 5 M NaOH solution, the reactor block was sealed and heated to 180 °C within 1 h. The temperature was held for 96 h and then cooled to room temperature within 6 h. The green solid was centrifuged and redispersed in 20 mL of water (this process was repeated two times with water and three times with ethanol). The resulting green solid was dried in air at 70 °C.

Synthesis of Cr-MIL-101-Cl and Cr-MIL-101-Br. The starting materials CrO_3 (198 mg, 1.25 mmol) and TA-Cl/TA-Br (1.25 mmol) were introduced into a 40 mL Teflon reactor. After the addition of 5 mL of demineralized water and 76.5 μL (2.50 mmol) of concentrated HCl, the reactor was sealed and heated to 180 °C within 1 h. The temperature was held for 120 h and then cooled to room temperature within 6 h. The green solid was centrifuged and redispersed in 20 mL of water (this process was repeated two times with water and three times with ethanol). The resulting green solid was dried in air at 70 °C.

Postsynthetic Modification of Cr-MIL-101-Br-NO_2 to Cr-MIL-101-Br-NH_2. Cr-MIL-101-Br-NO_2 (60 mg) was suspended in 15 mL of ethanol, and 1.2 g of $SnCl_2 \cdot 2H_2O$ was added. The mixture was stirred for 6 h at 70 °C. The green suspension was centrifuged and redispersed in 20 mL of concentrated HCl. The solid was centrifuged again and redispersed in 20 mL of demineralized water (this process was repeated two times with water and three times with ethanol). The resulting green solid was dried in air at 70 °C.

Sample Treatment Prior to NMR Measurements. Due to the paramagnetic properties of the chromium species in the Cr-MIL-101 derivatives, the direct solid-state NMR measurement is not easily accomplished. To establish the molar ratio of the incorporated linker molecules and possible decomposition products, solution NMR spectroscopy was carried out. After the decomposition of the Cr-MIL-101 compounds in aqueous NaOH, the precipitated $Cr(OH)_3$ was removed by filtration. After the pH value was adjusted to pH ≈ 3, the terephthalic acid species were extracted with diethyl ether. After the solvent was removed in vacuo and dissolved the solid in 5% $NaOD/D_2O$ solution, the ^1H NMR spectra were recorded. Systems containing sulfoterephthalic acid were treated slightly different. After the $Cr(OH)_3$ was removed by filtration, the pH was adjusted to pH ≈ 3, and the water was evaporated at 70 °C. The solid was dissolved in 5% $NaOD/D_2O$ for solution NMR measurements. The relative amounts of linker molecules incorporated into the final Cr-MIL-101 derivative were calculated from the integrals of the ^1H NMR signals, which are characteristic for each terephthalic acid derivative.

■ RESULTS AND DISCUSSION

High-Throughput Screening. For the synthesis of the new functionalized Cr-MIL-101 derivatives, three different metal sources were used: $Cr(NO_3)_3 \cdot 9H_2O$ from which Cr-MIL-101 originally was obtained,[17] $CrCl_3$ from which Cr-MIL-101-NO_2 can be synthesized,[15] and CrO_3 which was reported as the metal source for Cr-MIL-101-SO_3H.[21] Initially, a high-throughput metal screening experiment was carried out in order to determine where the most crystalline Cr-MIL-101 phases can be found. On the basis of previous results on functionalized Cr-MIL-101 derivatives, long reaction times (96–120 h) were chosen.[15,21] In addition to single-linker systems, mixed-linker systems containing equimolar mixtures of functionalized terephthalic acid derivatives were also investigated (Figure 2).

Using CrO_3 as the metal source yielded predominantly X-ray amorphous products (Figure 3 and Supporting Information Table S1). Besides Cr-MIL-53 and Cr-MIL-88, four pure Cr-MIL-101 phases and mixtures thereof were also formed. It is notable that the system with pure monosodium-2-sulfoterephthalic acid did not form Cr-MIL-101-SO_3H as described elsewhere.[21] Although the original synthesis was carried out in a 100 mL autoclave, the syntheses in this study are carried out in 2 mL reactors. This unexpected behavior could be due to the change of the reactor size because different surface to volume ratios lead to changes in the heating profile, which also affects the solubility of the starting materials.

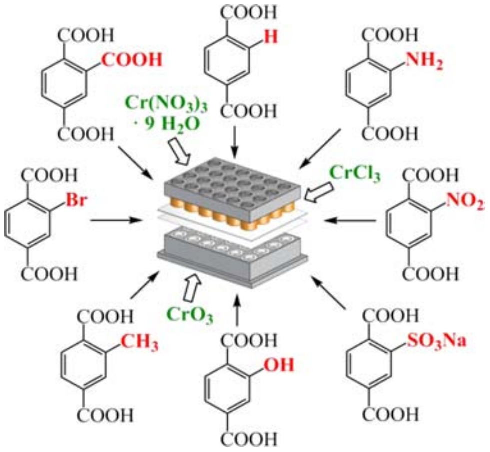

Figure 2. Schematic representation of terephthalic acid derivatives and chromium sources used in the high-throughput screening to obtain single- and mixed-linker Cr-MIL-101 compounds.

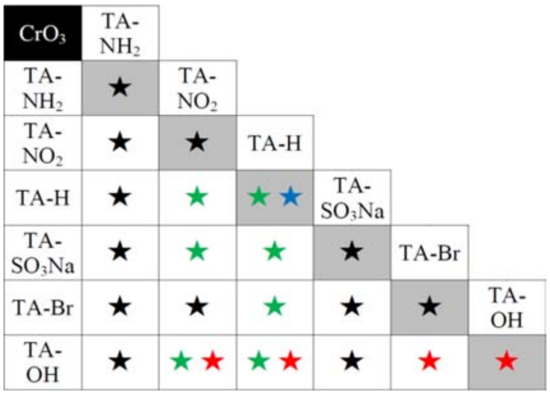

CrO_3	TA-NH_2	TA-NO_2	TA-H	TA-SO_3Na	TA-Br	TA-OH
TA-NH_2	⬛					
TA-NO_2	⬛	⬛				
TA-H	⬛	🟩	🟩 🟦			
TA-SO_3Na	⬛	🟩	🟩	⬛		
TA-Br	⬛	⬛	🟩	⬛	⬛	
TA-OH	⬛	🟩 🟥	🟩 🟥	⬛	🟥	🟥

Figure 3. Results of the high-throughput metal screening experiment with CrO_3 as the metal source (green = Cr-MIL-101, black = X-ray amorphous, red = Cr-MIL-53, blue = Cr-MIL-88). The shaded fields denote the single-linker systems.

Using $Cr(NO_3)_3 \cdot 9H_2O$ as the metal source gave eight pure crystalline Cr-MIL-101 phases (Figure 4 and Supporting Information Table S2). Similar to the results using CrO_3, X-ray amorphous products and Cr-MIL-53, but no Cr-MIL-88, were observed. The effect of employing miniaturized reactors is also observed in the single-linker system using terephthalic acid. In addition to Cr-MIL-101, small amounts of Cr-MIL-53 were observed (Supporting Information Figure S1). This could also be due to the extended reaction time of 96 h. In the original synthesis of the Cr-MIL-101, a reaction time of 8 h was used.

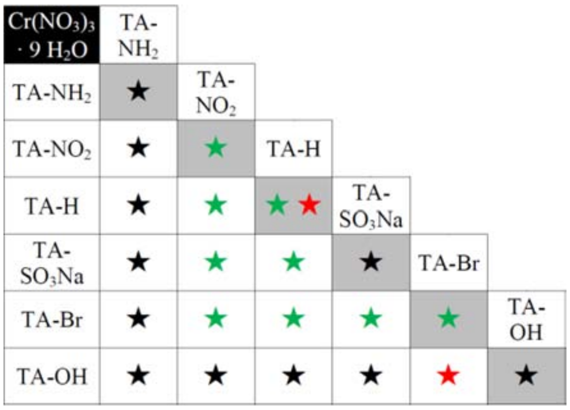

$Cr(NO_3)_3$ · 9 H_2O	TA-NH_2	TA-NO_2	TA-H	TA-SO_3Na	TA-Br	TA-OH
TA-NH_2	⬛					
TA-NO_2	⬛	🟩				
TA-H	⬛	🟩	🟩 🟥			
TA-SO_3Na	⬛	🟩	🟩	⬛		
TA-Br	⬛	🟩	🟩	🟩	🟩	
TA-OH	⬛	⬛	⬛	⬛	🟥	⬛

Figure 4. Results of the high-throughput metal screening experiment with $Cr(NO_3)_3 \cdot 9H_2O$ (green = Cr-MIL-101, black = X-ray amorphous, red = Cr-MIL-53). The shaded fields denote the single-linker systems.

Using $CrCl_3$ as the metal source resulted in a large number of single- and mixed-linker Cr-MIL-101 derivatives (Figure 5). Furthermore, the number of functionalized terephthalic acids used was extended, and methylterephthalic acid (TA-CH_3) and trimellitic acid (TA-COOH) were also employed. In this system, the majority of products were crystalline Cr-MIL-101 derivatives (Figure 5, Supporting Information Table S3). The

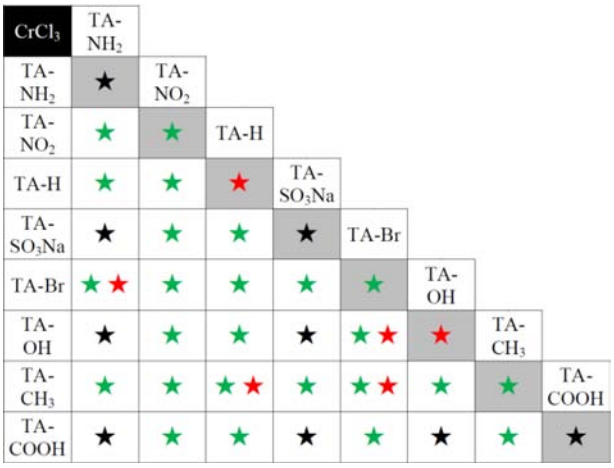

$CrCl_3$	TA-NH_2	TA-NO_2	TA-H	TA-SO_3Na	TA-Br	TA-OH	TA-CH_3	TA-COOH
TA-NH_2	⬛							
TA-NO_2	🟩	🟩						
TA-H	🟩	🟩	🟥					
TA-SO_3Na	⬛	🟩	🟩	⬛				
TA-Br	🟩🟥	🟩	🟩	🟩	🟩			
TA-OH	⬛	🟩	🟩	⬛	🟩🟥	🟥		
TA-CH_3	🟩	🟩	🟩🟥	🟩	🟩🟥	🟩	🟩	
TA-COOH	⬛	🟩	🟩	⬛	🟩	⬛	🟩	⬛

Figure 5. Results of the high-throughput metal screening experiment using anhydrous $CrCl_3$ as the metal source (green = Cr-MIL-101, black = X-ray amorphous, red = Cr-MIL-53). The shaded fields denote the single-linker systems. In contrast to the results of using CrO_3 or $Cr(NO_3)_3 \cdot 9H_2O$ as the metal source, mainly Cr-MIL-101 derivatives were obtained.

mixed-linker systems with TA-Br and TA-NO_2 yielded highly crystalline Cr-MIL-101 derivatives (Supporting Information Figure S2, Figure 6). Although the use of TA-NO_2 resulted exclusively in the formation of Cr-MIL-101 derivatives (Figure 6), very small impurities of Cr-MIL-53 derivatives were observed when TA-Br was employed (Supporting Information Figure S2).

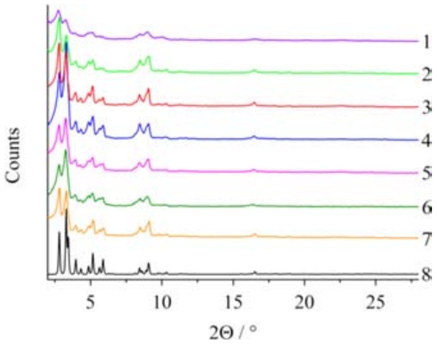

Figure 6. PXRD patterns of reaction products obtained in the high-throughput screening with TA-NO_2 compared to the simulated pattern of Cr-MIL-101 (8, black): Cr-MIL-101-NO_2-NH_2 (1, violet), Cr-MIL-101-NO_2-H (2, light green), Cr-MIL-101-NO_2-SO_3H (3, red), Cr-MIL-101-NO_2-Br (4, blue), Cr-MIL-101-NO_2-OH (5, pink), Cr-MIL-101-NO_2-CH_3 (6, dark green), and Cr-MIL-101-NO_2-COOH (7, orange).

SEM measurements were carried out to determine the morphology of the reaction products. Cr-MIL-101 crystals are easily recognized by their octahedral shape; thus, byproducts can easily be detected (Supporting Information Table S5). The observed crystal shapes support, in general, the results of the PXRD measurements. Mostly phase-pure products are obtained. The products that contain a byproduct according to the PXRD data exhibit crystals of different morphologies. In the micrographs of Cr-MIL-101-Cl, Cr-MIL-101-CH_3, and Cr-MIL-101-Br-H, particles of different morphology are observed. Because no crystalline impurities were detected in the PXRD patterns, they are present only in small amounts or they are not crystalline.

Because we started with equimolar mixtures of TA-X linker molecules in the synthesis, the relative amount of linker molecules incorporated into the final Cr-MIL-101 structure gives information on the reactivity of these derivatives. Solution ^1H NMR spectroscopy of single- and mixed-linker Cr-MIL-101 samples was carried out to quantify the relative amounts of linker molecules incorporated and to determine if the decomposition of the linker molecules had taken place under the harsh reaction conditions. These results are summarized in Figure 7, Supporting Information Table S6, and Supporting Information Figure S14–S20. In some systems, small amounts (ca. 1–2%) of terephthalic acid (TA-H) were detected, which is due to the presence of TA-H impurities in the commercially available functionalized terephthalic acid derivatives (Supporting Information Table S5).

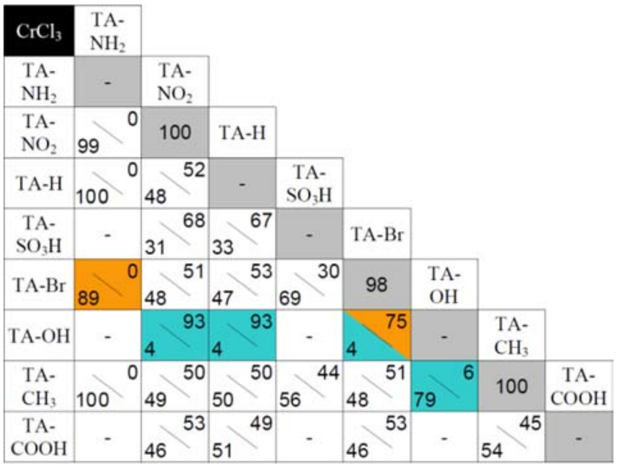

$CrCl_3$	TA-NH_2	TA-NO_2	TA-H	TA-SO_3H	TA-Br	TA-OH	TA-CH_3	TA-COOH
TA-NH_2	-							
TA-NO_2	0 99	100						
TA-H	0 100	52 48	-					
TA-SO_3H	-	68 31	67 33	-				
TA-Br	0 89	51 48	53 47	30 69	98			
TA-OH	-	93 4	93 4	-	75 4	-		
TA-CH_3	0 100	50 49	50 50	44 56	51 48	6 79	100	
TA-COOH	-	53 46	49 51	-	53 46	-	45 54	-

Figure 7. Molar ratios of the incorporated linker molecules in the Cr-MIL-101 derivatives obtained when $CrCl_3$ was used as the metal source. Molar ratios are based on the results of solution ^1H NMR experiments (orange = presence of 2-chloroterephthalic acid, blue = presence of 3-hydroxybenzoic acid, gray = single-linker systems). Full details are given in Supporting Information Table S6.

In comparison to the recently reported results on the formation of Cr-MIL-101-NH_2, which was feasible using an OH-assisted hydrothermal synthesis carried out at 150 °C for 12 h,[18] the use of pure TA-NH_2 or TA-OH in the synthesis of Cr-MIL-101 leads exclusively to X-ray amorphous products under the studied reaction conditions. Their use of mixed-linker Cr-MIL-101 derivatives in the formation does not (TA-NH_2) or does only in small amounts (TA-OH) lead to the incorporation of these linker molecules in the final structure. Therefore, control experiments without adding the metal source to the reaction mixture were carried out. These show that TA-NH_2 and TA-OH undergo a decomposition reaction, and 3-aminobenzoic acid and 3-hydroxybenzoic acid, respectively, are formed (Figure 8). This reaction has been reported already in 1877 for "oxodicarboxylic acids" and can be explained by the decarboxylation at elevated temperatures during the synthesis.[26] Additionally, in the systems TA-Br/TA-NH_2 and TA-Br/TA-OH, the chlorine derivative TA-Cl was observed in the final Cr-MIL-101 derivative. This occurrence must be due to the use of $CrCl_3$ as the metal source and the partial substitution in acidic reaction milieu.

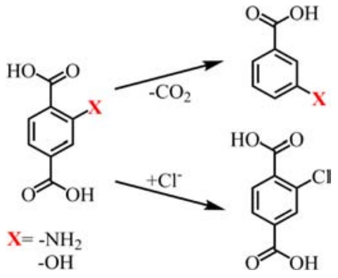

Figure 8. Decarboxylation (top) and nucleophilic substitution (bottom) of 2-aminoterephthalic acid and 2-hydroxyterephthalic acid taking place at a reaction temperature of 180 °C.

Synergistic effects are observed when TA-COOH is used in the synthesis of mixed-linker Cr-MIL-101 derivatives. Although the use of TA-COOH as single-linker leads only to X-ray amorphous products, the use of equimolar mixtures with TA-H, TA-NO_2, TA-Br, or TA-CH_3 leads to the incorporation of both linker molecules in an almost equimolar ratio each.

The use of TA-SO_3Na resulted in the formation of mixed-linker Cr-MIL-101 derivatives when TA-H, TA-Br, TA-NO_2, and TA-CH_3 were employed. According to the results of the NMR measurements, the incorporated molar ratio deviates substantially from the one used in the reaction mixture. With the exception of the synthesis using TA-CH_3, the final products contain ca. 1/3 TA-SO_3H, and no side reactions of the linker molecules could be detected (Supporting Information Table S6). Two possible reasons are the very good solubility of the monosodium-2-sulfoterephthalic acid or its lower reactivity.

Single-Linker Cr-MIL-101 Derivatives. In addition to mixed-linker Cr-MIL-101 derivatives, the direct synthesis of single-linker derivatives was also investigated. Therefore, the terephthalic acid derivatives TA-X with X = CH_3, F, Cl, Br, and I were studied. The PXRD patterns of the reaction products are presented in Figure 9. These newly incorporated functional groups could be valuable for PSM reactions.

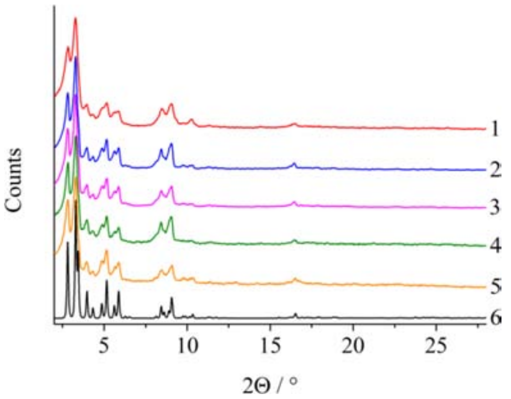

Figure 9. Powder pattern of the single-linker Cr-MIL-101 compounds compared to the simulated pattern of Cr-MIL-101 (6, black): Cr-MIL-101-CH_3 (1, red), Cr-MIL-101-F (2, blue), Cr-MIL-101-Cl (3, pink), Cr-MIL-101-Br (4, green), and Cr-MIL-101-I (5, orange).

Cr-MIL-101-CH_3 was obtained from $CrCl_3$ and TA-CH_3 using the 2 mL reactor system. PXRD measurements demonstrated the formation of crystalline Cr-MIL-101 without any crystalline impurity (Figure 9, 1). After decomposition of the framework structure and extraction of the linker molecules, ^{1}H NMR spectroscopy showed that only TA-CH_3 was incorporated and did not undergo any site reactions (Supporting Information Figure S3). Additionally, in the IR spectrum, the methyl C−H stretching vibrations can be found between 2900 and 2974 cm^{-1} (Supporting Information Figure S4).

Also, halogenated Cr-MIL-101 derivates were directly obtained from the corresponding functionalized terephthalic acid derivatives. Cr-MIL-101-F was obtained from a reaction mixture of $CrCl_3$ and TA-F upon addition of sodium hydroxide and using the 2 mL reactor system. The addition of sodium hydroxide leads to deprotonation of TA-F and, thus, increases the solubility. In contrast, Cr-MIL-101-F was recently reported to be accessible by a two-step procedure starting with Cr-MIL-101-NH_2 and carrying out a Schiemann reaction.[24] PXRD measurements of the directly synthesized Cr-MIL-101-F reaction product demonstrate the phase purity (Figure 9, 2). Using IR spectroscopy, we found the characteristic C−F stretching vibration at 1234 cm^{-1} (Supporting Information Figure S5).[27] To demonstrate that TA-F is incorporated, we employed solution ^{1}H NMR spectroscopy. In addition to the TA-F, only traces of unfunctionalized terephthalic acid (2%) were found (Supporting Information Figure S6). Cr-MIL-101-Cl was obtained in large amounts in the 40 mL reactor system starting from CrO_3, TA-Cl, and concentrated HCl. No crystalline byproducts were formed (Figure 9, 3), and the characteristic C−Cl stretching vibration is observed at 1050 cm^{-1} in the IR spectrum (Supporting Information Figure S7).[27] ^{1}H NMR measurements show the sole incorporation of TA-Cl (Supporting Information Figure S8). Cr-MIL-101-Br could also be obtained in large amounts in the 40 mL reactor system starting from CrO_3, TA-Br, and concentrated HCl. PXRD measurements reveal that Cr-MIL-101-Br was obtained without crystalline impurities (Figure 9, 4). Employing IR spectroscopy, we observed the characteristic C−Br stretching vibration at 1042 cm^{-1} (Supporting Information Figure S9).[27] Solution ^{1}H NMR spectroscopy demonstrated the presence of small amounts of terephthalic acid (2%). (Supporting Information Figure S10).

The attempt to synthesize Cr-MIL-101-I directly from $Cr(NO_3)_3\cdot 9H_2O$, TA-I, and concentrated HCl resulted in the formation of a crystalline compound denoted Cr-MIL-101-I. No crystalline impurities could be detected (Figure 9, 5). The detailed characterization of the incorporated linker molecules by ^{1}H NMR measurements revealed an unexpected linker composition (Figure 10). In addition to TA-I, the majority of linker molecules were shown to be TA-NO_2, although TA-Cl and TA-H were also found (molar ratio TA-I/TA-NO_2/TA-Cl/TA-H = 0.18/1/0.25/0.06). In the IR spectrum of Cr-MIL-101-I, the C−I stretching vibration (1049 cm^{-1}) and the C−Cl stretching vibration (1073 cm^{-1}) were found (Supporting Information Figure S11).[27]

The incorporation of the different linker molecules can be explained by side reactions taking place during the synthesis. Iodine is known to be a very good leaving group, and the in situ formation of TA-Cl and TA-NO_2 is due to nucleophilic substitution reactions occurring at the elevated reaction temperature. Cr-MIL-101-I has recently been shown to be accessible by postsynthetic modification starting with Cr-MIL-101-NH_2 via Sandmeyer reaction.[24]

Postsynthetic Modification. Because the direct incorporation of TA-NH_2 in mixed-linker Cr-MIL-101 derivatives has not been successful, the postsynthetic modification route was chosen. On the basis of the results of the synthesis of Cr-MIL-

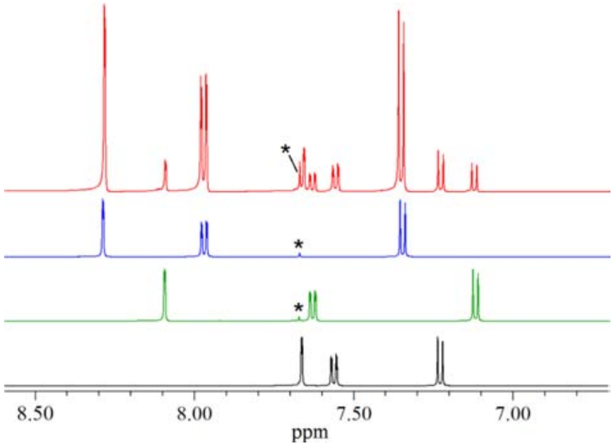

Figure 10. 500 MHz ^{1}H NMR spectra of the extracted linker molecules from Cr-MIL-101-I obtained from the direct synthesis using TA-I (red). In addition, the NMR spectra of pure 2-nitroterephthalic acid (blue), 2-iodoterephthalic acid (green), and 2-chloroterephthalic acid (black) are presented. The signal of the unfunctionalized terephthalic acid is marked with a star.

101-NH_2 starting from Cr-MIL-101-NO_2, the mixed-linker derivative Cr-MIL-101-Br-NO_2 was used for a postsynthetic modification reaction.[15] In cases where all nitro groups are accessible for the reduction, a Cr-MIL-101 derivative containing only TA-Br and TA-NH_2 should be achievable. PXRD measurements prove the preservation of the crystallinity during these harsh reaction conditions (Figure 11).

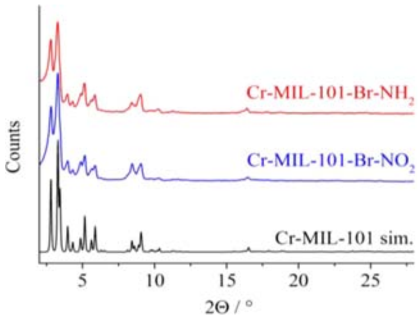

Figure 11. PXRD pattern of Cr-MIL-101-Br-NH_2 compared to that of Cr-MIL-101-Br-NO_2 and the simulated pattern of Cr-MIL-101.

Solution ^{1}H NMR measurements show the successful modification of the nitro groups (Figure 12). In the spectrum of the extracted linker molecules, only signals of TA-Br and TA-NH_2 can be found; additionally, a small signal corresponding to the presence of terephthalic acid is observed. It can thus be concluded that all nitro groups in Cr-MIL-101-Br-NO_2 are accessible and were quantitatively reduced.

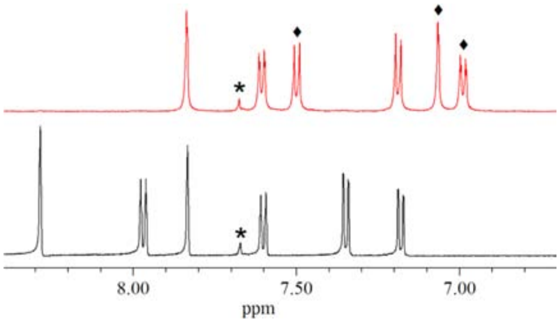

Figure 12. 500 MHz ^{1}H NMR spectra of the extracted linker molecules from Cr-MIL-101-Br-NH_2 (red) and Cr-MIL-101-Br-NO_2 (black). The signal which is characteristic for terephthalic acid is marked with a star, and the signals of TA-NH_2 are marked with diamonds.

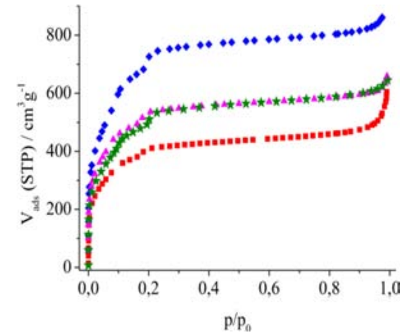

Figure 13. N_2 adsorption isotherms of the single-linker Cr-MIL-101 derivatives: Cr-MIL-101-F (blue diamonds), Cr-MIL-101-Cl (pink triangles), Cr-MIL-101-Br (green stars), and Cr-MIL-101-CH_3 (red squares).

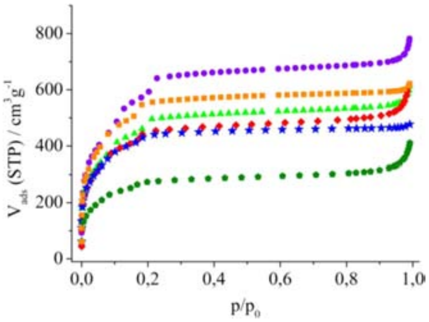

Figure 14. N_2 adsorption isotherms of the mixed-linker Cr-MIL-101 derivatives: Cr-MIL-101-Br-NH_2 (violet circles), Cr-MIL-101-Br-COOH (orange squares), Cr-MIL-101-Br-NO_2 (light green triangles), Cr-MIL-101-Br-H (red diamonds), Cr-MIL-101-Br-SO_3H (blue stars), and Cr-MIL-101-Br-CH_3 (dark green pentagons).

N_2 Sorption Measurements. The results of the sorption measurements of the single- and selected mixed-linker Cr-MIL-101 derivatives are presented in Figures 13 and 14, Table 1, and the Supporting Information (Figures S12 and S13). Literature values of previously reported Cr-MIL-101 compounds are given for comparison. The observed S_{BET} values of the single- and mixed-linker Cr-MIL-101 derivatives fall within the range of values previously reported. An exception is the small value observed for Cr-MIL-101-Br-CH_3, which is due to the presence of small amounts of impurities observed in the PXRD and SEM measurements. In all sorption isotherms, the characteristic two-step curve shape is observed, which is due to the filling of two cages of different sizes.[17] The S_{BET} values of the halogen-functionalized Cr-MIL-101-X derivatives decrease with increasing weight, although the values observed for the -Cl and -Br differ only slightly. There is no clear trend comparing the single-linker with the corresponding mixed-linker systems. The S_{BET} values for Cr-MIL-101-Br-NH_2 falls between the values of the single-linker systems, whereas for Cr-MIL-101-Br-SO_3H and Cr-MIL-101-Br-NO_2, the values observed are below and above, respectively, the corresponding single-linker systems.

Table 1. Specific Surface Areas (S_{BET}) and Micropore Volumes of the Single-Linker Cr-MIL-101-X Derivatives with TA-X[a] and Mixed-Linker Cr-MIL-101-Br-Y Derivatives with TA-Y[b]

Cr-MIL-101	S_{BET} [$m^2\ g^{-1}$]	V_{mic} [$cm^3\ g^{-1}$]	V_{tot} [$cm^3\ g^{-1}$]	reference
-H	2367−4100	2.0(1)[e]		15, 21, 29
-F	2282[c]	1.20[c]		this work
-F	1619[d]		1.26[d]	24
-Cl	1720[c]	0.87[c]		this work
-Br	1631[c]	0.87[c]		this work
-I	1431[d]		1.19[d]	24
-CH_3	1467[c]	0.68[c]		this work
-NH_2	2313[c]	1.09[c]		15
-NH_2	2070[d]		2.26[d]	24
-NO_2	1425[c]	0.75[c]		15
-SO_3H	1915			21
-Br-NH_2	1900[c]	1.03[c]		this work
-Br-COOH	1870[c]	0.89[c]		this work
-Br-NO_2	1696[c]	0.80[c]		this work
-Br-H	1574[c]	0.74[c]		this work
-Br-SO_3H	1549[c]	0.70[c]		this work
-Br-CH_3[f]	991[c]	0.45[c]		this work

[a] X = CH_3, F, Cl, Br. [b] Y = CH_3, NH_2, COOH, NO_2, H, SO_3H. [c] Specific surface area (S_{BET}) calculated using the Rouquerol approach;[28] micropore volume (V_{mic}) determined at $p/p_0 = 0.5$. [d] Specific surface area (S_{BET}) calculated in the p/p_0 range of 0.05−0.1; total volume (V_{tot}) calculated taking the data at $p/p_0 = 0.99$. [e] Evaluated using the Dubinin−Radushkevich equation. [f] Small impurities of Cr-MIL-53 present in the sample.

CONCLUSIONS

We have demonstrated the successful formation of new single- and mixed-linker functionalized Cr-MIL-101 derivatives. A metal screening experiment with three different chromium sources revealed the influence of the metal ion source on the formation of Cr-MIL-101-based compounds. For the setup used in this study, the best results were obtained using $CrCl_3$ as the metal source. Similar systematic studies have previously demonstrated that the solubility of linker molecules is a crucial factor for the formation of Fe- and Al-MIL-101.[19,20] Hence, under the studied reaction conditions, the solubility of $CrCl_3$ seems to be optimal for the formation of Cr-MIL-101 derivatives.

We were able to obtain the new single-linker Cr-MIL-101-CH_3 derivative. The use of halogenated terephthalic acids in the hydrothermal synthesis yielded the halogenated Cr-MIL-101 derivatives Cr-MIL-101-F, Cr-MIL-101-Cl, and Cr-MIL-101-Br. Cr-MIL-101-I could not be obtained directly by hydrothermal synthesis due to nucleophilic substitution reactions taking place during the synthesis. A number of mixed-linker Cr-MIL-101 compounds were obtained. A synergetic effect was observed during the synthesis of Cr-MIL-101-COOH-Y compounds. Only certain combinations with other functional groups yielded the desired reaction product, and the corresponding single-linker compound Cr-MIL-101-COOH could not be obtained. In the future, the new single-linker as well as the mixed-linker compounds could be used for further postsynthetic modification reactions. As an example, we have shown that the -NO_2 groups in Cr-MIL-101-Br-NO_2 can be selectively reduced to yield Cr-MIL-101-Br-NH_2 without any loss of crystallinity.

ASSOCIATED CONTENT

Supporting Information

Tables with ratios of incorporated linker molecules of mixed-linker Cr-MIL-101-derivatives, PXRD patterns, and IR spectra. Solution ^1H NMR spectra of selected reaction products. This material is available free of charge via the Internet at http://pubs.acs.org.

AUTHOR INFORMATION

Corresponding Author

*E-mail: stock@ac.uni-kiel.de.

Notes

The authors declare no competing financial interest.

§E-mail: dirk.devos@biw.kuleuven.be.

ACKNOWLEDGMENTS

We appreciate support from the Deutsche Forschungsgemeinschaft (DFG, SPP 1362) and Prof. Dr. Sönnichsen (University of Kiel) for NMR measurements.

REFERENCES

(1) Thematic issues: Metal−Organic Frameworks: (a) *Chem. Soc. Rev.* **2009**, Issue 5; *Chem. Rev.* **2012**, Vol. *112*.

(2) Sonnauer, A.; Hoffmann, F.; Fröba, M.; Kienle, L.; Duppel, V.; Thommes, M.; Serre, C.; Férey, G.; Stock, N. *Angew. Chem., Int. Ed.* **2009**, *48*, 3791.

(3) Furukawa, H.; Ko, N.; Go, Y. B.; Aratani, N.; Choi, S. B.; Choi, E.; Özgür Yazaydin, A.; Snurr, R. Q.; O'Keeffe, M.; Kim, J.; Yaghi, O. M. *Science* **2010**, *329*, 424.

(4) (a) Tanabe, K. K.; Cohen, S. M. *Chem. Soc. Rev.* **2011**, *40*, 498. (b) Biswas, S.; Ahnfeldt, T.; Stock, N. *Inorg. Chem.* **2011**, *50*, 9518.

(5) (a) Vermoortele, F.; Ameloot, R.; Vimont, A.; Serre, C.; De Vos, D. E. *Chem. Commun.* **2011**, *47*, 1521. (b) Horcajada, P.; Surblé, S.; Serre, C.; Hong, D.-Y.; Seo, Y.-K.; Chang, J.-S.; Grenèche, J.-M.; Margiolaki, I.; Férey, G. *Chem. Commun.* **2007**, 2820.

(6) (a) Latroche, M.; Surblé, S.; Serre, C.; Mellot-Draznieks, C.; Llewellyn, P. L.; Lee, J.-H.; Chang, J.-S.; Jhung, S. H.; Férey, G. *Angew. Chem., Int. Ed.* **2006**, *45*, 8227. (b) Suh, M. P.; Park, H. J.; Prasad, T. K.; Lim, D.-W. *Chem. Rev.* **2012**, *112*, 782.

(7) (a) Maes, M.; Alaerts, L.; Vermoortele, F.; Ameloot, R.; Couck, S.; Finsy, V.; Denayer, J. F. M.; De Vos, D. E. *J. Am. Chem. Soc.* **2010**, *132*, 2284. (b) Maes, M.; Vermoortele, F.; Alaerts, L.; Couck, S.; Kirschhock, C. E. A.; Denayer, J. F. M. *J. Am. Chem. Soc.* **2010**, *132*, 15277.

(8) Horcajada, P.; Chalati, T.; Serre, C.; Gillet, B.; Sebrie, C.; Baati, T.; Eubank, J. F.; Heurtaux, D.; Clayette, P.; Kreuz, C.; Chang, J.-S.; Hwang, Y. K.; Marsaud, V.; Bories, P.-N.; Cynober, L.; Gil, S.; Férey, G.; Couvreur, P.; Gref, R. *Nat. Mater.* **2010**, *9*, 172.

(9) (a) Jeremias, F.; Khutia, A.; Henninger, S. K.; Janiak, C. *J. Mater. Chem.* **2012**, *22*, 10148. (b) Seo, Y.-K.; Woon, J. W.; Lee, J. S.; Hwang, Y. K.; Jun, C.-H.; Chang, J.-S.; Wuttke, S.; Bazin, P.; Vimont, A.; Daturi, M.; Bourrelly, S.; Llewellyn, P. L.; Horcajada, P.; Serre, C.; Férey, G. *Adv. Mater.* **2012**, *24*, 806.

(10) Deng, H.; Doonan, C. J.; Furukawa, H.; Ferreira, R. B.; Towne, J.; Knobler, C. B.; Wang, B.; Yaghi, O. M. *Science* **2010**, *327*, 846.

(11) Devic, T.; Horcajada, P.; Serre, C.; Salles, F.; Maurin, G.; Moulin, B.; Heurtaux, D.; Clet, G.; Vimont, A.; Grenèche, J.-M.; Le Ouay, B.; Moreau, F.; Magnier, E.; Filinchuk, Y.; Marrot, J.; Lavalley, J.-C.; Daturi, M.; Férey, G. *J. Am. Chem. Soc.* **2010**, *132*, 1127.

(12) Horcajada, P.; Salles, F.; Wuttke, S.; Devic, T.; Heurtaux, D.; Maurin, G.; Vimont, A.; Daturi, M.; David, O.; Magnier, E.; Stock, N.; Filinchuk, Y.; Popov, D.; Riekel, C.; Férey, G.; Serre, C. *J. Am. Chem. Soc.* **2011**, *133*, 17839.

(13) Reinsch, H.; Waitschat, S.; Stock, N. *Dalton Trans.* **2013**, *42*, 4840.

(14) Cohen, S. M. *Chem. Rev.* **2012**, *112*, 970.

(15) Bernt, S.; Guillerm, V.; Serre, C.; Stock, N. *Chem. Commun.* **2011**, *47*, 2838.

(16) Volkringer, C.; Cohen, S. *Angew. Chem., Int. Ed.* **2010**, *49*, 4644.

(17) Férey, G.; Mellot-Draznieks, C.; Serre, C.; Millange, F.; Dutour, J.; Surblé, S.; Margiolaki, I. *Science* **2005**, *309*, 2040.

(18) Lin, Y.; Kong, C.; Chen, L. *RSC Adv.* **2012**, *2*, 6417.

(19) Stavitski, E.; Goesten, M.; Juan-Alcañiz, J.; Martinez-Joaristi, A.; Serra-Crespo, P.; Petukhov, A. V.; Gascon, J.; Kapteijn, F. *Angew. Chem.* **2011**, *123*, 9798.

(20) Bauer, S.; Serre, C.; Devic, T.; Horcajada, P.; Marrot, J.; Férey, G.; Stock, N. *Inorg. Chem.* **2008**, *47*, 7568.

(21) Akiyama, G.; Matsuda, R.; Sato, H.; Takata, M.; Kitagawa, S. *Adv. Mater.* **2011**, *23*, 3294.

(22) Goesten, M. G.; Juan-Alcaniz, J.; Ramos-Fernandez, E. V.; Sai Sankar Gupta, K. B.; Stavitski, E.; van Bekkum, H.; Gascon, J.; Kapteijn, F. *J. Catal.* **2011**, *281*, 177.

(23) Modrow, A.; Zargarani, D.; Herges, R.; Stock, N. *Dalton Trans.* **2012**, *41*, 8690.

(24) Jiang, D.; Keenan, L. L.; Burrows, A.; Edler, K. J. *Chem. Commun.* **2012**, *48*, 12053.

(25) Stock, N. *Microporous Mesoporous Mater.* **2010**, *129*, 287.

(26) Burkhardt, G. A. *Chem. Ber.* **1877**, *10*, 144.

(27) Socrates, G. *Infrared Characteristic Group Frequencies*, 2nd ed.; Wiley: Chichester, U.K., 1994.

(28) Rouquerol, J.; Llewellyn, P.; Rouquerol, F. *Stud. Surf. Sci. Catal.* **2007**, *160*, 49.

(29) Henschel, A.; Gedrich, K.; Kraehnert, R.; Kaskel, S. *Chem. Commun.* **2008**, 4192.